Peer-reviewed version available at *Nanomaterials* **2019**, *9*, 1303; doi:10.3390/nano9091303

Article

New Evidence of the Bidentate Binding Mode in 3-MBA Protected Gold Clusters: Analysis of Aqueous 13–18 kDa Gold-Thiolate Clusters by HPLC-ESI-MS Reveals Special Compositions $Au_n(3\text{-MBA})_p$, (n = 48 – 67, p = 26-30)

David M. Black,[1] M. Mozammel Hoque,[1*] Germán Placencia-Villa, [1,2] Robert L Whetten[1*]

[1]Department of Physics & Astronomy, University of Texas, San Antonio, TX 78249, USA
[2]Department of Biology, University of Texas, San Antonio, TX 78249, USA
*Correspondence: whettenz60@gmail.com; mohammad.hoque64@gmail.com

Abstract: Gold clusters protected by 3-MBA ligands (MBA = mercaptobenzoic acid, -SPhCO$_2$H) have attracted recent interest for their unusual structures and advantageous ligand-exchange and bioconjugation properties. Azubel *et al*. first determined the core structure of an Au_{68}-complex, which was estimated to have 32 ligands (3-MBA groups). To explain the exceptional structure-composition and reaction properties of this complex, and its larger homologs, Tero *et al*. proposed a "dynamic stabilization" via carboxyl O-H--Au interactions. Herein, we report the first results of an integrated LC/MS analysis of unfractionated samples of gold / 3-MBA clusters, spanning the narrow size range 13.4 to 18.1 *kDa*. Using high-throughput procedures adapted from bio-macromolecule analyses, we show that integrated capillary HPLC-ESI-MS, based upon aqueous-methanol mobile phases and ion-pairing reverse-phase chromatography, can separate *several* major components from the nanoclusters mixture that may be difficult to resolve by standard native gel electrophoresis due to their similar size and charge. For each component, one obtains a well-resolved mass spectrum, nearly free of adducts or signs of fragmentation. A consistent set of molecular mass determinations is calculated from detected charge-states tunable from 3- (or lower), to 2+ (or higher). One thus arrives at a series of new compositions (n, p) specific to the Au/3-MBA system. The smallest major component is assigned to the previously unknown (48, 26); the largest one is evidently (67, 30), *vs*. the anticipated (68, 32). Various explanations for this discrepancy are considered. A prospective is given for the *several* members of this novel series, along with a summary of the advantages and present limitations of the micro-scale integrated LC/MS approach to characterize such metallic-core macro-molecules, and their derivatives.

Keywords: 3-MBA; gold clusters; ESI-MS; HPLC-MS; bidentate binding

1. Introduction

This work on the 3-MBA protected gold clusters, or cluster compounds, has been motivated by the following circumstances, in brief:

(i) A *Science* paper from 2014 identified a medium-sized (68, 32) 3-MBA gold cluster and determined its structure by an HREM-based statistical algorithm.[1]

(ii) It has been proposed[2-4] that this ligand has a different 'binding mode' than its sister 4-MBA (pMBA), which is better understood especially thanks to Vergara *et al.*'s recent subatomic resolution of the (146, 57) compound.[5]

(iii) Previous attempts by the Tsukuda group to analyze these by ESI-MS are limited in scope, as the spectra obtained are "too broad" (unresolved), i.e. inadequate to establish the composition, e.g. is it truly Au_{68} (as the HREM reconstruction indicates)? What is the true ligand count (supplied by computational modeling)?

(iv) According to our best evidence, the main component is (67, 30), rather than the previously published (68, 32), and smaller main component is (48, 26). These unusual numbers, and indeed the

entire graph of observed composition number (p vs. n), are consistent with the theoretical and experimental (nuclear magnetic resonance, NMR) proposition of a special (bidentate) mode of 3-MBA binding. This trend-line (dependency) is in accord with the idea that as the size increases, the decreasing curvature (of the core's surface) increases the propensity for the bidentate mode. Asymptotically, for flat surfaces (self-assembled monolayers, SAMS) may be dominated by this binding mode.

Noble metal clusters, especially of gold and its intermetallic compounds, form highly stable complexes with thiolate and other pseudo-halide ligands. These are often called "monolayer protected clusters" (MPCs), because of their relation to the analogous self-assembled monolayers (SAMs) on planar or extended electrodes.[6-8] They have attracted special attention because of their nobility[9] (tolerance to air, moisture, and light; bio-compatibility, etc.); for their facile modification via ligand exchange reactions;[10-12] for high-contrast detection, whether visual/optical or in X-ray and electron scattering;[13] and for the fascination and potential utility of their strongly size-dependent optical, electrical and structure-bonding properties.[14-16]

By now, much evidence has accumulated to suggest that many of these MPCs may be obtained in high yield as pure macromolecular substances of definite composition[17-18] and structure-bonding characteristics,[19-21] as opposed to the more usual metal colloidal or nanoparticle[9] substances that often show heterogeneity. Such proven structural uniformity of MPCs is essential to precision-intensive applications, as well as to all fundamental physicochemical understanding. The most compelling demonstrations are the cases of total structure determination by single crystal X-ray[22] or electron diffraction methods,[23] which for gold-thiolates have recently been extended to MPCs as large as $Au_{146}(pMBA)_{57}$ (aqueous)[5] and $Au_{279}(TBBT)_{84}$ (nonaqueous).[24]

Azubel *et al*.[1] determined the core structure of an Au_{68}-complex by cryo-TEM, which was estimated to have 32 ligands (3-MBA groups). Tero *et al*.[4] proposed a "dynamic stabilization" mechanism via carboxyl O-H--Au interactions to explain its structure, composition and reaction properties, as well as those of its larger homologs.[2-3]

Many reports have discussed the challenge of adequately characterizing samples of novel MPCs, particularly in the early stages of identifying the main compounds or components of a mixture, as discussed elsewhere.[25-26] Our approach here has been to adapt a method—electrospray ionization (ESI)-coupled high performance liquid chromatography mass spectrometry (HPLC-MS)—established earlier for bio-macromolecules of a similar size (or mass) and surface chemistry as the MPCs under investigation.[27] Specifically, the larger Au/MBA clusters have many (~24-60) acid-terminated ligands,[3] and so are presumed to exist in aqueous solution at normal (or higher) pH as poly-anions (plus respective counter-cations). For this case, long experience with oligonucleotides (DNA or RNA), composed of similar number, ~24 – 60 base-sugar-phosphate repeats) seem most instructive.

Our aims in the present work have been (i) to determine whether the unusual solution-phase characteristics of the Au/3-MBA clusters will permit them to yield to analyze by the ESI-coupled LC-MS methods that have recently improved the analysis of Au-pMBA clusters ranging from small oligomers and clusters (25, 18) and (36, 24) to the larger species (102, 44), (130, 50) and (144, 60);[27] (ii) to examine whether ion-pairing agents will work similarly to enable both high-resolution LC separations and reduced-fragmentation ESI-ToF (time-of-flight) mass spectra; (iii) to provide some insight into the powerful selection principles underlying the results in refs. 1-4; (iv) to search for minor or hidden components (new compositions) as semi-stable or transition MPCs; (v) to provide additional evidence pertaining to the 'bidentate' or dynamical carboxyl-gold interactions described in ref. 4.

Herein, we report the first results of an ESI-coupled LC-MS analysis of unfractionated samples of Au/3-MBA clusters that span a narrow mass range, 13.4 – 18.2 kDa. Using procedures adapted from oligonucleotide analyses, we show that integrated capillary HPLC-ESI-MS, based upon aqueous-methanol mobile phases and ion-pairing reverse-phase chromatography, can separate *at least two* major components (and several minor ones) that are present in all sources. For each component, a well-resolved mass spectrum, nearly free of adducts or signs of fragmentation, allows determination of a consistent assignment of molecular masses, as calculated from detected charge-

states tunable from 3- (or lower), to 2+ (or higher). One thus arrives at a set of proposed compositions (*n*, *p*), as characteristic of the Au/3-MBA system. The smaller major component is assigned to the previously unknown (48, 26); the larger one is assigned to (67, 30), *vs*. the anticipated (68, 32).

2. Materials and Methods

2.1. Synthesis. The size-uniform sample prepared at the University of Texas at San Antonio by Germán Placencia-Villa (*GPV*) for this work are synthesized according to a modified Brust-Schiffrin approach described elsewhere.[1] In brief, a stirred solution of 3:1 3-MBA – $HAuCl_4$ solution was allowed to equilibrate for 16 hours under basic conditions in 30% methanol prior to the cluster forming reduction reaction initiated by the addition of sodium borohydride. This altered method has been shown to produce uniformly sized clusters, as opposed to production of many discretely sized particles.

2.2. 3-MBA/Au System Characterization. Characterization of molecular nanoparticle preparations is carried out by a variety of methods for characterization of the system of interest. Size-exclusion,[28] gel-permeation,[29] and thin-layer chromatography,[30] gel-electrophoresis,[31] reversed-phase,[32] and hydrophobic interaction[33] liquid chromatography have all been extensively used as an essential analytical tools for characterization of such nanoclusters. These methods separate the various components of a mixture according to one or more physical and/or chemical attributes including differences in size, polarity, hydrophobic character, and electrophoretic mobility (related size-to-charge ratio). Ion-pairing can be combined with reversed-phase LC for analysis of acidic and basic clusters.[34] Separation methods may be used alone for sample fractionation or in conjunction with various detectors.

Analysis of nanoclusters by these methods is only possible for those samples exhibiting a certain degree of modal- or multi-modal distribution—with each mode showing minimal variance. Samples that exhibit a continual distribution, as is the case with nanoparticles exceeding approximately 3-nm core diameter, are not amenable to LC or MS analysis. 'Magic-number' nanocluster preparations are good candidates for characterization by liquid chromatography and mass spectrometry because these clusters form in a multi-modal fashion, with only a few compositions exhibiting a high degree of stability. The LC-MS data acquired from these samples may be used to assign specific cluster identity as well as for semi-quantitative determination of each of the components present in a sample. Aqueous nanoparticles, like those investigated here, are of interest because of their potential application in medical and life sciences.[2-3]

2.2.1. Coupled Chromatography – ESI-MS. In the present work discussed here, efforts were focused to determine whether the 3-MBA/Au systems were amenable to analysis by HPLC-ESI-MS in the same way as previously observed for the analogous 4-MBA/Au systems (aka p-MBA/Au). Specifically of interest was the possibility of ion-pairing with triethylammonium cations (TEAH+)[27] for retention and separation of these poly-acid clusters *via* reversed phase chromatography. Also, of interest was an understanding of the effectiveness of this ion-pairing strategy for electrospray ionization (ESI) and if the necessary conditions could be implemented to supported determination of cluster compositions with some degree of clarity by minimizing fragmentation. Successful implementation of HPLC-MS to these systems may help reveal 'hidden components'[35]—not otherwise known or detectable by native PAGE gel-electrophoresis. Any evidence to support or refute the proposed 'bidentate' bonding (H-bonding of carboxyl to Au) is also of interest in these studies.

Although gel-electrophoresis is a standard technique for analysis of nanoparticle preparations, it is a relatively course size separation method. An exact determination of size and uniformity requires confirmation by a secondary analytical technique since it is possible for the components having different sizes, shapes, or charges to share the same, or similar, electrophoretic mobilities.

2.2.2. HP-LC–ESI-MS sample preparation. Obtained Au/3-MBA samples were either re-dispersed or diluted—if a solid or solution, respectively—approximately 10x in appropriate solution. LC separation was performed with coupled electrospray time-of-flight mass spectrometry detection (ToF-MS). Separations were carried out on a C_{18} stationary phase using gradient methods whereby

the initial mobile phase composition was replaced one with a higher organic concentration in a linear fashion over a period of twenty minutes. Mobile phases were prepared containing 400 mM hexfluoroisopropanol (HFIP) - 15 mM triethylamine (TEA), TEA-HFIP *or* 10 mM triethylammonium acetate (TEAA) in ddH_2O (mobile phase A) and methanol (mobile phase B). The separation behavior of the nanoparticles predominantly depends on the selected combination of stationary phase, mobile phase, gradient, and mobile phase modifier. Starting from the conditions used to obtain satisfactory separation and ionization of the larger p-MBA/Au MPCs, the gradient and modifier selection were varied to find conditions for satisfactory separations. Near-baseline separation of the various components is crucial to provide differentiation and correlation between the various MS signal observed which aids MS interpretation, and reduces the possibilities for ion-suppression artifacts. The gradient method can be adapted to produce greater separation between components and the mobile phase modifier is essential for good chromatographic performance compatible with acceptable electrospray ionization. Solution phase ion-pairing effectively neutralizes the MBA's carboxylate ($-COO^-$) group by association with $TEAH^+$, enhancing the interaction of the mercaptobenzoic acid ligands with the C_{18} stationary phase.

3. Results

Recent reports have demonstrated the possibility of producing uniformly-sized batches of 3-mercaptobenzoic acid (MBA) protected nanoparticles.[1-4] Smaller nanoparticles, or nanoclusters, are noteworthy for their interesting properties, and because certain stoichiometries (i.e., gold-to-ligand ratios) form in abundance due to their relatively higher thermodynamic stability.[4, 36] This phenomenon makes it possible to produce specific nanomolecular particles in abundance. However, because there exist various "magic-number" sizes (e.g., Au_{25}, Au_{38}, Au_{68}, Au_{102}, Au_{144}, etc.), nanoclusters preparations may still exhibit heterogeneity or mixtures varying from one batch to the next. These improved synthetic procedures make it possible to produce size-focused preparations of nanoparticles thus enabling the production of a higher quality product. Synthetic procedures such as these, in tandem with analytical methods that can be used to characterize these preparations, may provide the needed capabilities for development of various nanoparticle applications. The 3-MBA/Au systems demonstrate 'certain advantages' over other thiolates (organic or hydrophobic) for purposes of ligand exchange and conjugation, as well as bio-applications.

Figure 1 shows negative-ionization (-ESI) LC-MS mode data acquired following on the sample (prepared by the size-uniform synthesis procedure) provided by M. Azubel, as prepared at the Stanford University. Two dominant components are readily identified: (67, 30; 17.8 kDa) and (48, 26; 13.4 kDa). These appear at the short (long) retention times and high (low) mass ends of the spectrum.

Preprints (www.preprints.org) | NOT PEER-REVIEWED | Posted: 26 August 2019 doi:10.20944/preprints201908.0263.v1

Peer-reviewed version available at Nanomaterials 2019, 9, 1303; doi:10.3390/nano9091303

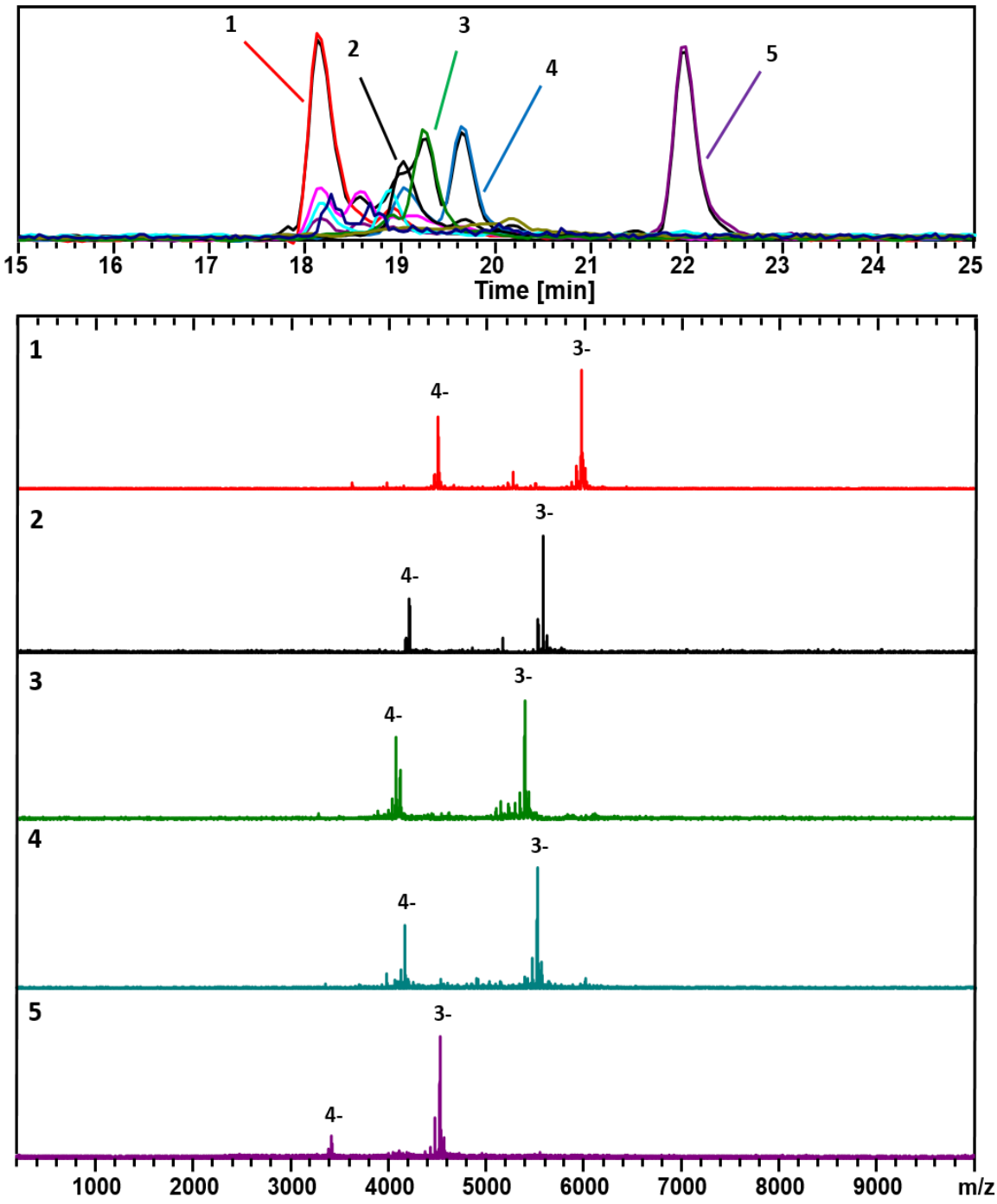

Figure 1. ESI-coupled LC-MS analysis of Au / 3-MBA clusters from the Azubel-preparation. Detection is set for negative ions, under conditions that generate mainly 3- and 4- charge states. The top frame shows the chromatograms, i.e. the base peak chromatogram (m/z 100 – 10000), and an extracted-ion chromatogram (EIC) for each component identified. The color-coded EIC chromatographic peaks track with the coded and numbered mass spectra listed herein with compositions assigned as follows: (**1, Red**) (67, 30), 17.8 kDa; (2, Black) (60, 31), 16.6 kDa; (3, Green) (58, 30), 16.0 kDa; (4, Blue) (60, 30), 16.4 kDa; and (**5, Purple**) (48, 26), 13.4 kDa. The fine-structure of the $[67, 30]^{3-}$ complexes is presented in Figure S1.

Figure 2 shows results from analysis of the same sample, obtained in the positive-ionization (+ESI) LC-MS mode. Mass spectra are shown for each of the 5 major components (67, 30; 18.1 kDa), (60, 31; 16.9 kDa), (58, 30; 16.2 kDa), (60, 30; 16.6 kDa), and (48, 26; 13.6 kDa. These are considered

also in assigning the compositions listed in Figure 1. In both cases, 10 mM TEAA was used as the ion-pairing agent to facilitate the ionization process.

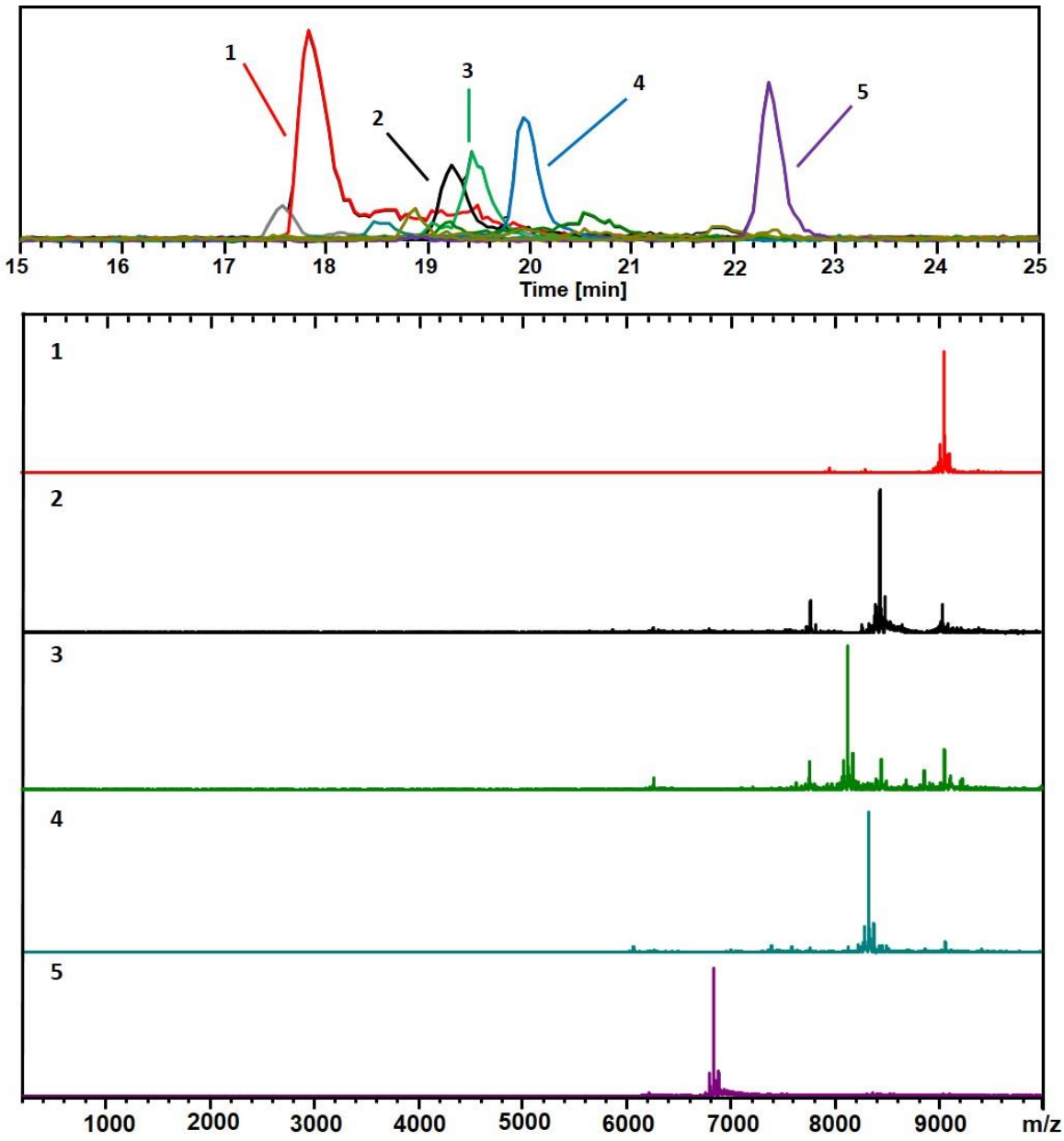

Figure 2. As in Figure 1, but with positive (ESI+) mode for detection. This analysis shows mainly 2+ charge-states. The black trace corresponds to the base peak chromatogram (m/z 100 – 10000). The color-coded EIC chromatographic peaks track with the coded and numbered mass spectra listed herein with compositions assigned as follows: (1, Red) (67, 30), 18.1 kDa; (2, Black) (60, 31), 16.9 kDa; (3, Green) (58, 30), 16.2 kDa; (4, Blue) (60, 30), 16.6 kDa; and (5, Purple) (48, 26), 13.6 kDa. Fine structure of the $[67, 30]^{2+}$ complexes are presented in Figure S2.

Figures 3 and 4 show two analyses with two different ion-pairing agents TEAA and TEA-HFIP, respectively of a separate preparation (*GPV*) of 3-MBA clusters.

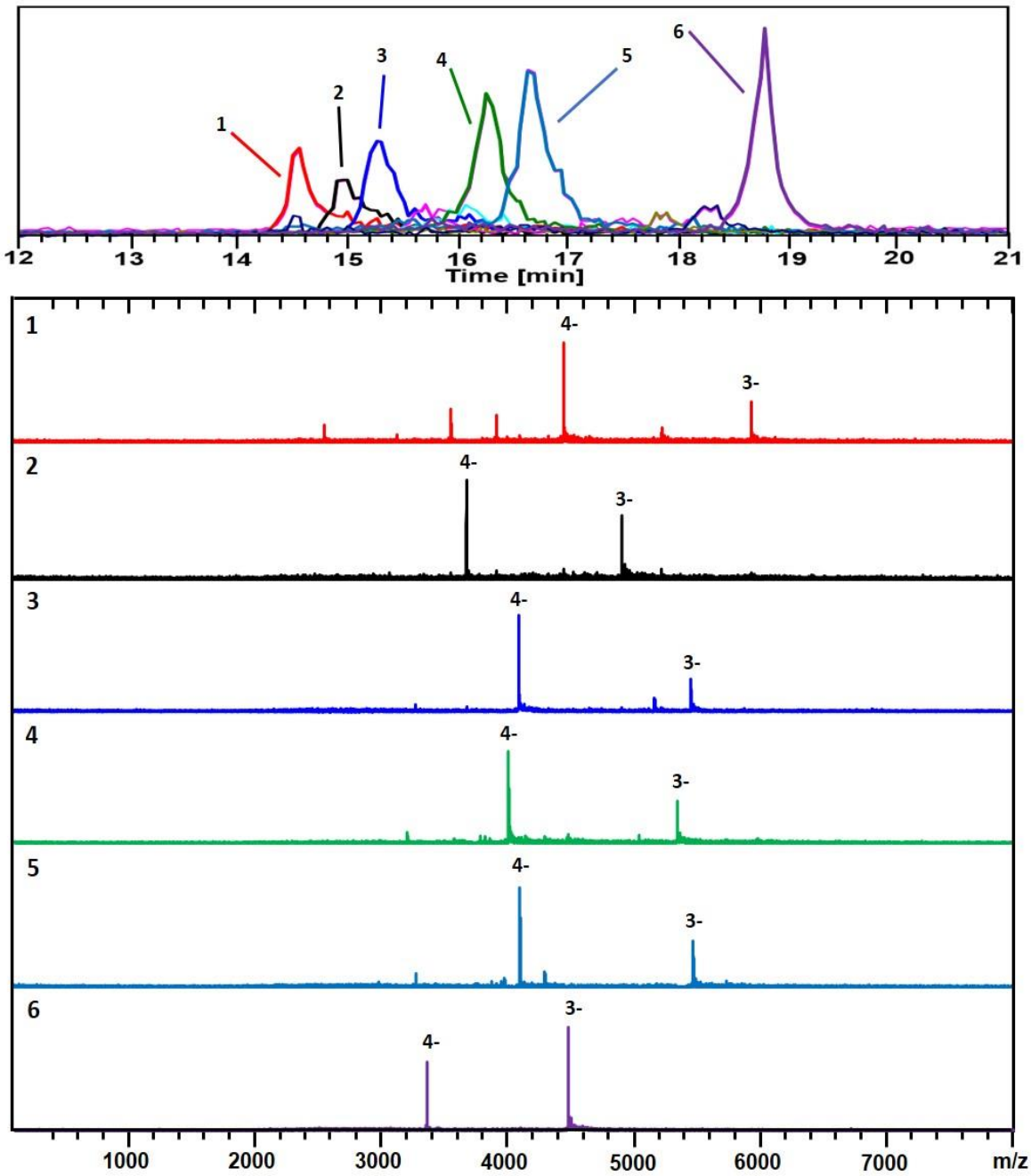

Figure 3. Analysis of a second preparation (*GPV*) of Au/3-MBA clusters. Negative ionization mode (-ESI) detection shows mainly 3- & 4- charge-states. The black trace corresponds to the base peak chromatogram (m/z 100 – 8000). The color-coded EIC chromatographic peaks track with the coded and numbered mass spectra listed herein, with compositions assigned as follows: (1, Red) (67, 30), 17.8 kDa; (2, Black) (53, 28), 14.7 kDa; (3, Blue) (59, 31), 16.3 kDa; (4, Green) (58, 30), 16.0 kDa; (5, Light Blue) (60, 30), 16.4 kDa; and (6, Purple) (48, 26), 13.4 kDa. For the singly charged (z = 1-) of the same sample see Figure S3 and S4. The polyacrylamide gel-electrophoresis (PAGE) analysis and corresponding HPLC-ESI-MS chromatogram are presented in Figure S4.

Preprints (www.preprints.org) | NOT PEER-REVIEWED | Posted: 26 August 2019 doi:10.20944/preprints201908.0263.v1

Peer-reviewed version available at Nanomaterials 2019, 9, 1303; doi:10.3390/nano9091303

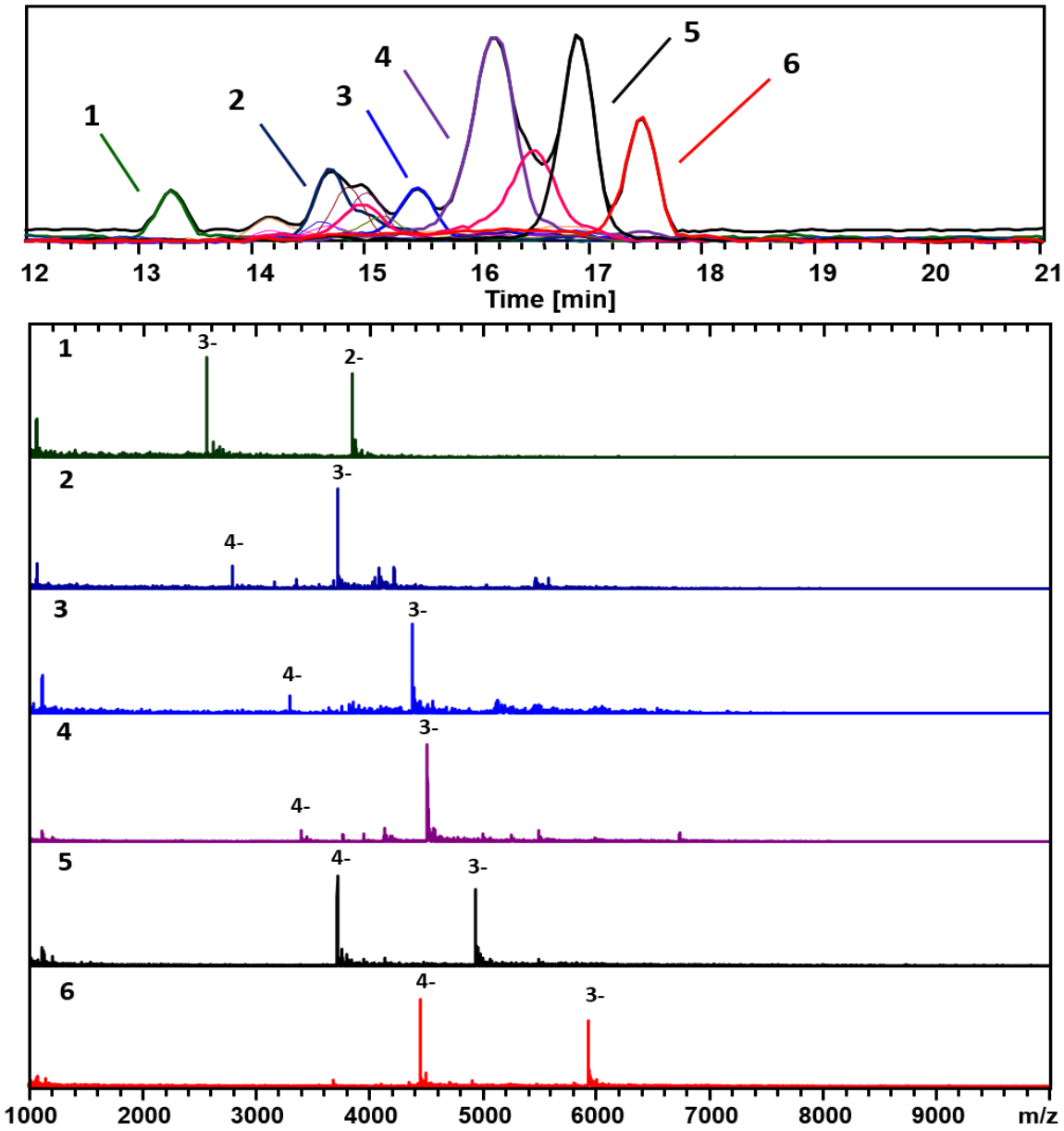

Figure 4. Analysis of the second preparation of 3-MBA clusters using TEA–HFIP mobile phase buffer composition. Negative ionization mode used for analysis, mainly 3- and 4- charge-states. The black trace corresponds to the base peak chromatogram (m/z 1000 – 10000). The color-coded EIC chromatographic peaks track with coded and numbered mass spectra listed and compositions assigned as follows: (1, Dark green) (25, 18), 7.7 kDa; (2, Dark Blue) (38, 24), 11.1 kDa; (3, Blue) (46, 26), 13.0 kDa; (4, Purple) (48, 26), 13.4 kDa; (5, Black) (53, 28), 14.7 kDa; and (6, Red) (67, 30), 17.8 kDa.

Besides the main components (67, 30; 17.8 kDa) and (48, 26; 13.4 kDa) identified as in Figures 1 and 2 (*Azubel*'s sample), several other minor ones (25, 18; 7.7 kDa), (38, 24; 11.1 kDa) are identified with our ESI-MS method, especially at smaller mass. Figure 4 shows results for the same sample analyzed using a combination of a more volatile weak acid HFIP than acetic, and TEA. Interestingly, while the components observed in each analysis are essentially identical, the order of elution is significantly altered for the two modifiers. The TEAA modifier produces chromatography whereby the larger clusters generally elute first, followed by smaller ones. The TEA-HFIP reverses this general trend such that smaller clusters elute first followed by larger ones.

Figure 5 contains a comparison among the mass spectra above (Figures. 1-4), as they pertain to the putative "Au_{68}(3-MBA)$_{32}$" compound (calculated mass of 18.3-kDa), and also to an extract from

the mass spectrum provided in Reference 1. In negative-ion detection, as appropriate to polyacids, the evidence all points toward 17.8-kDa, the mass of (67, 30). In positive-ion detection, where TEAH+ adducts provide the charge, the mass of 18.1-kDa also agrees with (67,30), assuming triple-adduction, i.e. 3 TEAH+, in which case the [67, 30] complex carries an intrinsic (core) charge of 1-.

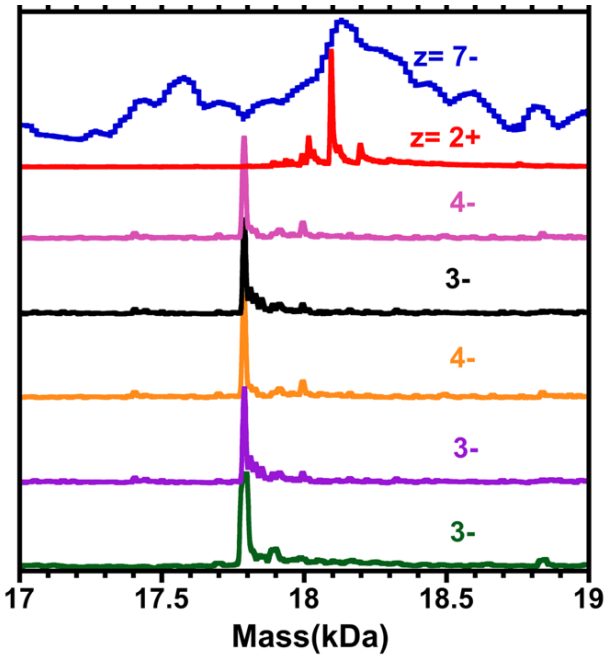

Figure 5. Comparison of deconvoluted mass spectra in the region of the 17.8-kDa compound, putatively "Au_{68}(3-MBA)$_{32}$", vs. the ESI-MS of reference 1 (blue curve at top). Depicted are selected portions of the ESI mass spectra of gold cluster samples, in which the independent variable has been converted from (m/z) scale to total mass (kDa), using the charge (z) assignments indicated in Figure 2 (red), Figure 4 (pink and purple), Figure 1 (orange and black), and Figure 3 (dark green). Note that in the case of positive ion mode (z = 2+), the peak is shifted higher by ~ +0.3 kDa, consistent with three (3) $TEAH^+$ adducts, to the $[67,30]^{1-}$ complex. [Mass of $TEAH^+$= 101 Da.]

Figure 6 shows plots of the various chemical compositions observed for each of the different samples analyzed here. Although a number of different compositions were observed for each sample, a clear difference between the size-uniformity of the two samples can be observed. When a long equilibration prior to reduction is carried out, a much narrower range of cluster sizes is formed. If the procedure is varied—even slightly—to reduce this time period, a wider range of cluster sizes is formed, that is supported by the recent reported "captamino", a base side, thiolated gold clusters in the size range 25-144 number of Au, or even larger. [17,18] In the Figure 3, cluster compositions ranging from (47, 26) to (71, 34) are observed; whereas in Figure 4, compositions ranging from (25, 18) to (67, 30) are observed.

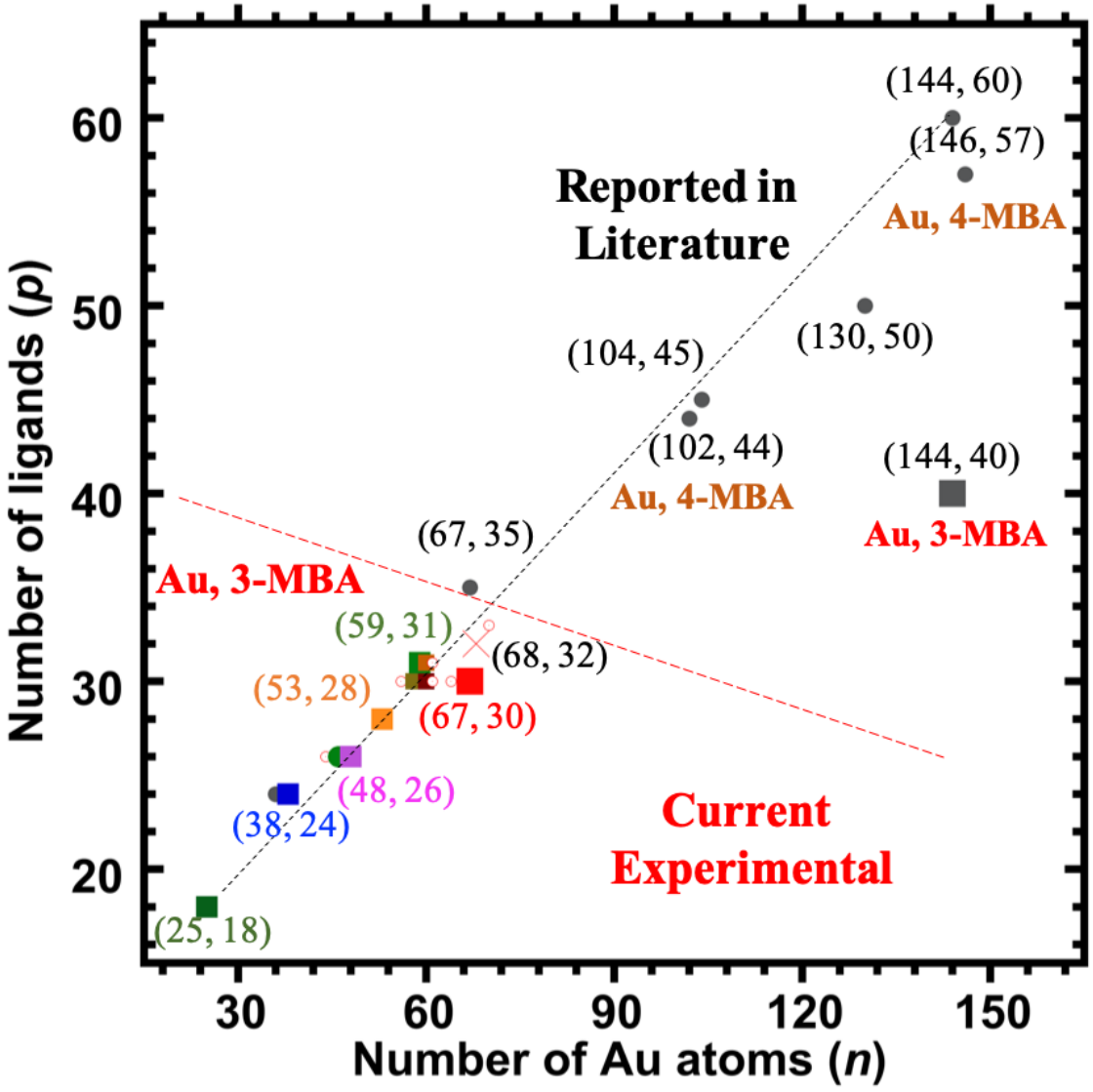

Figure 6. Number of ligands (p) vs number of Au atoms (n) found in this work on the $Au_n(3\text{-MBA})_p$, ($n = 48 – 67$, $p = 26\text{-}30$) and reported in literature to see the trends. Legend: symbols designate whether the component identified was detected prominently (colored large square) and for both samples under all ESI-coupled LC/MS conditions, or not (small hollow red circle); red cross represents the expected (68, 32) clusters, grey large square represents 3-MBA thiolated larger (144, 40) clusters, whereas small grey circles (filled) represent reported different composition of other thiolated clusters, for example 4-MBA (a sister molecule of 3-MBA) thiolated $Au_{146}(4\text{-MBA})_{57}$.

4. Discussion

4.1. General Remarks

As mentioned in the Introduction section, our general objective in this research has been to advance the analytical chemistry of thiolate-protected gold clusters. Specifically, we have aimed to adapt the standard HPLC-ESI-MS methodology, as applied for example to oligonucleotides, which are acidic (poly-anionic), developing optimized strategies to gold clusters protected by a monolayer of thiolate ligands with terminal *(solution-exposed)* acidic groups. The recent progress reported by Black et al. includes HPLC-ESI-MS identification of a long series of Au-pMBA clusters as large as (146, 57),[5] or as small as (25, 18) and (36, 24). By use of a suitable ion-pairing agent (TEA+), well resolved

mass spectra could be obtained under gentler conditions (to reduce poly-anion fragmentation in electrospray ionization) and nearly free from alkali-ion and solvent adducts.[27] In a related work, silver-lipoate clusters [29, 12]$^{(3-)}$ have been effectively resolved, where lipoate acts as a bidentate (di-thiolate) ligand with a terminal carboxylate ("thioctic acid").[37-38]

4.2. Contrasting 3-MBA (or meta-MBA) and 4-MBA (aka para-MBA)

In turning from the 4-MBA (pMBA) to 3-MBA (or "mMBA") ligands, one faces a more challenging analytical situation, as described most recently in a 2017 *ACS Nano* report of Tero *et al*.[4] as well as the earlier reports of Azubel *et al*.,[1-3] dating to the 2014 *Science* article:

- There has been no total-structure determination of any 3-MBA protected gold clusters.
- There has been no adequately resolved ESI-MS identification of any of these. No composition-determination by any standard analytical method.
- Electron microscopy (or diffraction) provides the gold structure and atom count, in both (2) reported cases. (Ligands / S-atoms are not located by this method). Models are then constructed that include the ligands, and these are tested (refined) by DFT computations.
- The compositions arrived at by these procedures (68, 32) and (144, ~40) are respectively distinctly and strikingly different from those determined previously for aliphatic ligands, (67, 35) and (144, 60), or for the more directly relevant water-soluble aromatic pMBA ligand (146, 57). [*The Figure 6 presents these compositions in graphical format*.]

In practice, (by the same HPLC-ESI-MS optimized procedures) we were able readily to obtain clear results on the samples believed to be dominated by the (68, 32), but not on the samples labeled as larger compounds (144, ~40). This is not particularly surprising for large polyanionic assemblies have a reputation for difficult ESI-MS analysis. For the same reason, presence of readily detectable smaller components, such as the major one assigned to (48, 26), or even the minor (25, 18) in one instance, is unsurprising, as their signal levels may be disproportionate to their concentration in solution.

Perhaps the major positive result of our work is the greatly improved (vs. 2014 Science report[1]) quality of ESI mass spectra, Figure 5, that led us to identify (67, 30) as the composition of the compound previously assigned to (68, 32). This is only a minor difference, amounting to a single gold atom and two (2) 3-MBA ligands, but could suggest a reinterpretation of its structure and bonding.

However, one should note that this suggested revision (reducing the ligand-count to 30 from 32) only serves *increase* its distinctiveness, as compared to the reference (aliphatic) case, i.e. (67, 35) vs. (67, 30). Now the 'ligand deficiency' (below) is five (5) rather than two (2), as indicated in Figure 6. The other components, and specifically the one identified as (48, 26), may also be interpreted within this same context of 'ligand deficiency'. Figure 6 shows that the important compositions (36, 24) and also (44, 28), for gold clusters protected by thiophenol-class thiolates, lie on a distinct 'curve'. Yet the smallest (minor) compound identified here as (25, 18) is the same regardless the of thiolate.

In the following, we suggest how the 'dynamical stabilization' model — a form of bidentate ligation — of Tero *et al*.[4] can be generalized, from the two cases {(68, 32), (144, ~40)} investigated by them, to account for the entire range of compositions identified and presented in the Figure 6. The dynamic-stabilization model (DSM)[4] was reported to account for the optical (FTIR) spectra as well as other analytical observations, in such a way that also explains the ligand-count deficiency and the lability of these two compounds when exposed to other (non-3-MBA) thiolates in solution. In particular, the basis for this model is described as follows:

- The vibrational FTIR spectra show in the carbonyl (C=O) stretching region "distinct peak[s] around 1730 cm^{-1}, observable only in 3-MBA-passivated clusters, and interpreted as the signal of the O=C−OH···Au interaction."[4]
- Molecular dynamics (MD) simulations were based on structure models for each cluster. "Visual inspection of MD trajectories revealed several weak interactions in the ligand layer and at the ligand−gold interface, such as formation of inter-ligand hydrogen bonds, inter-ligand π stacking (aromatic contacts), π−Au interaction where the aromatic ring lies "flat" on the gold

core, and hydrogen bonding-like O=C−OH···Au interaction when the hydroxyl group is rotated toward the gold core." "*We thus assigned the highest frequency observed for both* $Au_{144}(3\text{-MBA})_{\sim 40}$ *and* $Au_{68}(3\text{-MBA})_{32}$ *to the O=C−OH···Au interaction visualized* ... This interaction at the ligand−metal interface has not been reported before for any thiolate protected gold nanocluster."[4]

In the report, we have referred to any such interaction involving a second functional group (other than thiolate sulfur) as a "bidentate" bonding mode, whether the carboxyl group is protonated or de-protonated (as is more typical in solution-phase conditions, pH neutral or > 7).

First, the ligand-deficiency count, which ranges from 15-20 in the case of (144, ~40) to five (~5) for (67, 30), to perhaps a couple (2) in the case of (48, 26), and finally to zero (0) in (25, 18), is taken to represent *the number of ligands bound in a bidentate fashion*. Represented as a fraction of the whole: In the extreme case of (144, ~40), more than one-third of the ligands are bound in the bidentate mode. In the special case of (67, 30), one-sixth (5/30) are bidentate, and for (48, 26) only one-twelfth (2/26) are so indicated.

Second, as usual, the key step is to relate these fractions to the estimated curvature (1/R) of the structure as measured at its surface, where R is the radial distance at which the Au-S or Au-X bonds lie. A high curvature removes the driving force for bidentate coordination, because the steric constraints are greatly reduced (the position meta to sulfur should be well exposed to solvent and counter-cation).

For now, we leave this as a semiquantitative argument suitable for guiding further work on both the larger, or previously identified compounds, as well as the ones newly identified in this report. The need for this was well predicted in the closing remarks of Ref. 4: "Several currently unknown compositions and sizes of 3-MBA-protected gold nanoclusters will undoubtedly be found by variations of the known syntheses, which will open unexplored possibilities for applications of these materials in biolabeling, catalyzing biochemical reactions, imaging, detection, and theranostics."

Supplementary Materials: The following are available online at www.mdpi.com/xxx/s1; Figures S1-S4, fine-structure in the electrospray negative ionization mode mass spectrometric analysis of the (67, 30), complex $[67, 30]^{z-}$ in solution, electrospray positive ionization (ESI+) mass spectrometric analysis of the component identified as (67, 30), by HPLC-ESI-MS as in Figure 2, ESI-MS Analysis of *GPV* sample preparation, under conditions wherein mainly the singly charged (z = 1-) ions are detected, and the polyacrylamide gel electrophoresis (PAGE) and HPLC analyses of *GPV* sample preparation.

Acknowledgments: The co-authors thank Dr. Maia Azubel for providing the Stanford University samples used in this research, and Dr. Azubel and Prof. Roger Kornberg for their advice and encouragement. The Welch Foundation, via Grant AX-1857, provided financial support for this work.

Conflicts of Interest: The authors declare no conflict of interest.

References

1. Azubel, M.; Koivisto, J.; Malola, S.; Bushnell, D.; Hura, G. L.; Koh, A. L.; Tsunoyama, H.; Tsukuda, T.; Pettersson, M.; Häkkinen, H.; Kornberg, R. D., Electron microscopy of gold nanoparticles at atomic resolution. *Science* **2014**, *345* (6199), 909-912.
2. Azubel, M.; Kornberg, R. D., Synthesis of water-soluble, thiolate-protected gold nanoparticles uniform in size. *Nano Lett.* **2016**, *16* (5), 3348-3351.
3. Azubel, M.; Koh, A. L.; Koyasu, K.; Tsukuda, T.; Kornberg, R. D., Structure determination of a water-soluble 144-gold atom particle at atomic resolution by aberration-corrected electron microscopy. *ACS Nano* **2017**, *11* (12), 11866-11871.
4. Tero, T.-R.; Malola, S.; Koncz, B.; Pohjolainen, E.; Lautala, S.; Mustalahti, S.; Permi, P.; Groenhof, G.; Pettersson, M.; Hakkinen, H., Dynamic stabilization of the ligand–metal interface in atomically precise gold nanoclusters Au_{68} and Au_{144} protected by meta-mercaptobenzoic acid. *ACS Nano* **2017**, *11* (12), 11872-11879.
5. Vergara, S.; Lukes, D. A.; Martynowycz, M. W.; Santiago, U.; Plascencia-Villa, G.; Weiss, S. C.; de la Cruz, M. J.; Black, D. M.; Alvarez, M. M.; López-Lozano, X.; Barnes, C. O.; Lin, G.; Weissker, H.-C.; Whetten, R. L.; Gonen, T.; Yacaman, M. J.; Calero, G., MicroED Structure of $Au_{146}(p\text{-MBA})_{57}$ at Subatomic Resolution Reveals a Twinned FCC Cluster. *J. Phys. Chem. Lett.* **2017**, *8* (22), 5523-5530.

6. Kumara, C.; Hoque, M. M.; Zuo, X.; Cullen, D. A.; Whetten, R. L.; Dass, A., Isolation of a 300-kDa, $Au_{\sim 1400}$ Gold Compound, the Standard 3.6-nm Capstone to a Series of Plasmonic Nanocrystals Protected by Aliphatic-Like-Thiolates. *J. Phys. Chem. Lett.* **2018**, *9* (23), 6825–6832.
7. Aikens, C. M., Electronic and Geometric Structure, Optical Properties, and Excited State Behavior in Atomically Precise Thiolate-Stabilized Noble Metal Nanoclusters. *Acc. Chem. Res.* **2018**, *51*(12), 3065-3073.8.
8. Templeton, A. C.; Wuelfing, W. P.; Murray, R. W., Monolayer-Protected Cluster Molecules. *Acc. Chem. Res.* **2000,** *33* (1), 27-36.
9. Hoque, M. M.; Mayer, K. M.; Ponce, A.; Alvarez, M. M.; Whetten, R. L., Toward Smaller Aqueous-Phase Plasmonic Gold Nanoparticles: High-Stability Thiolate-Protected ~4.5 nm Cores. *Langmuir* **2019,** *35* (32), 10610-10617.
10. Huang, Z.; Ishida, Y.; Narita, K.; Yonezawa, T., Kinetics of Cationic-Ligand-Exchange Reactions in Au_{25} Nanoclusters. *J. Phys. Chem. C* **2018,** *122* (31), 18142-18150.
11. Ishida, Y.; Narita, K.; Yonezawa, T.; Whetten, R. L., Fully Cationized Gold Clusters: Synthesis of $Au_{25}(SR^{+})_{18}$. *J. Phys. Chem. Lett.* **2016,** *7* (19), 3718-3722.
12. Ishida, Y. S., J.; Akita, I.; Yonezawa, T., Ultrarapid Cationization of Gold Nanoparticles via a Single-Step Ligand Exchange Reaction. *Langmuir* **2018,** *34* (36), 10668-10672.
13. Gutierrez, E.; Powell, R.; Furuya, F.; Hainfeld, J.; Schaaff, T.; Shafigullin, M.; Stephens, P.; Whetten, R. Greengold, a giant cluster compound of unusual electronic structure. *Eur. Phys. J. D* **1999**, 9 (1), 647–651.
14. Nieto-Ortega, B.; Bürgi, T., Vibrational Properties of Thiolate-Protected Gold Nanoclusters. *Acc. Chem. Res.* **2018**, *51* (11), 2811-2819.
15. Hesari, M.; Ding, Z., A grand avenue to Au nanocluster electrochemiluminescence. *Acc. Chem. Res.* **2017**, *50* (2), 218-230.
16. Bauld, R.; Hesari, M.; Workentin, M. S.; Fanchini, G., Tessellated gold nanostructures from $Au_{144}(SCH_2CH_2Ph)_{60}$ molecular precursors and their use in organic solar cell enhancement. *Nanoscale* **2014**, *6* (13), 7570-7575.
17. Hoque, M. M.; Dass, A.; Mayer, K. M.; Whetten, R. L., Protein-Like Large Gold Clusters Based on the ω-Aminothiolate DMAET: Precision Thermal and Reaction Control Leading to Selective Formation of Cationic Gold Clusters in the Critical Size Range, n = 130–144 Gold Atoms. *J. Phys. Chem. C* **2019**, *123* (23), 14871-14879.
18. Hoque, M. M.; Black, D. M.; Mayer, K. M.; Dass, A.; Whetten, R. L., Base Side of Noble Metal Clusters: Efficient Route to Captamino-Gold, $Au_n(-S(CH_2)_2N(CH_3)_2)p$, n = 25–144. *J. Phys. Chem. Lett.* **2019**, *10* (12), 3307-3311.
19. Whetten, R. L.; Weissker, H.-C.; Pelayo, J. J.; Mullins, S. M.; López-Lozano, X.; Garzón, I. L., Chiral-Icosahedral (I) Symmetry in Ubiquitous Metallic Cluster Compounds (145A,60X): Structure and Bonding Principles. *Acc. Chem. Res.* **2019**, *52* (1), 34-43.
20. Sakthivel, N. A.; Dass, A., Aromatic Thiolate-Protected Series of Gold Nanomolecules and a Contrary Structural Trend in Size Evolution. *Acc. Chem. Res.* **2018**, *51* (8), 1774-1783.
21. Rambukwella, M.; Sakthivel, N. A.; Delcamp, J. H.; Sementa, L.; Fortunelli, A.; Dass, A., Ligand Structure Determines Nanoparticles' Atomic Structure, Metal-Ligand Interface and Properties. *Frontiers in Chemistry* 2018, 6 (330).
22. Yan, N.; Xia, N.; Liao, L.; Zhu, M.; Jin, F.; Jin, R.; Wu, Z., Unraveling the long-pursued Au_{144} structure by x-ray crystallography. *Science Advances* **2018**, *4* (10), eaat7259.
23. Hoque, M. M.; Vergara, S.; Das, P. P.; Ugarte, D.; Santiago, U.; Kumara, C.; Whetten, R. L.; Dass, A.; Ponce, A., Structural Analysis of Ligand-Protected Smaller Metallic Nanocrystals by Atomic Pair Distribution Function under Precession Electron Diffraction. *J. Phys. Chem. C* **2019,** *123* (32), 19894-19902.
24. Sakthivel, N. A.; Theivendran, S.; Ganeshraj, V.; Oliver, A. G.; Dass, A., Crystal Structure of Faradaurate-279: $Au_{279}(SPh\text{-}tBu)_{84}$ Plasmonic Nanocrystal Molecules. *J. Am. Chem. Soc.* **2017**, *139* (43), 15450-15459.
25. Chakraborty, I. P., T., Atomically Precise Clusters of Noble Metals: Emerging Link between Atoms and Nanoparticles. *Chem. Rev.* 2017, *117* (12), 8208-8271.
26. Jin, R.; Zeng, C.; Zhou, M.; Chen, Y., Atomically Precise Colloidal Metal Nanoclusters and Nanoparticles: Fundamentals and Opportunities. *Chemical Reviews* **2016,** *116* (18), 10346-10413.
27. Black, D. M.; Alvarez, M. M.; Yan, F.; Griffith, W. P.; Plascencia-Villa, G. n.; Bach, S. B.; Whetten, R. L., Triethylamine Solution for the Intractability of Aqueous Gold–Thiolate Cluster Anions: How Ion Pairing Enhances ESI-MS and HPLC of aq-$Au_n(pMBA)_p$. *J. Phys. Chem. C* **2016,** *121* (20), 10851-10857.

28. Knoppe, S.; Boudon, J.; Dolamic, I.; Dass, A.; Bürgi, T., Size exclusion chromatography for semipreparative scale separation of $Au_{38}(SR)_{24}$ and $Au_{40}(SR)_{24}$ and larger clusters. *Anal. Chem.* **2011**, *83* (13), 5056-5061.
29. Gies, A. P.; Hercules, D. M.; Gerdon, A. E.; Cliffel, D. E., Electrospray Mass Spectrometry Study of Tiopronin Monolayer-Protected Gold Nanoclusters. *J. Am. Chem. Soc.* **2007**, *129* (5), 1095-1104.
30. Ghosh, A.; Hassinen, J.; Pulkkinen, P.; Tenhu, H.; Ras, R. H.; Pradeep, T., Simple and efficient separation of atomically precise noble metal clusters. *Anal. Chem.* **2014**, *86* (24), 12185-12190.
31. Schaaff, T. G.; Knight, G.; Shafigullin, M. N.; Borkman, R. F.; Whetten, R. L., Isolation and selected properties of a 10.4 kDa gold: glutathione cluster compound. *J. Phys. Chem. B* **1998**, *102* (52), 10643-10646.
32. Choi, M. M.; Douglas, A. D.; Murray, R. W., Ion-pair chromatographic separation of water-soluble gold monolayer-protected clusters. *Anal. Chem.* **2006**, *78* (8), 2779-2785.
33. Niihori, Y.; Shima, D.; Yoshida, K.; Hamada, K.; Nair, L. V.; Hossain, S.; Kurashige, W.; Negishi, Y., High-performance liquid chromatography mass spectrometry of gold and alloy clusters protected by hydrophilic thiolates. *Nanoscale* **2018**, *10*(4), 1641-1649.
34. Niihori, Y.; Kikuchi, Y.; Shima, D.; Uchida, C.; Sharma, S.; Hossain, S.; Kurashige, W.; Negishi, Y., Separation of Glutathionate-Protected Gold Clusters by Reversed-Phase Ion-Pair High-Performance Liquid Chromatography. *Ind. Eng. Chem. Res.* **2017**, *56* (4), 1029-1035.
35. Alvarez, M. M.; Chen, J.; Plascencia-Villa, G.; Black, D. M.; Griffith, W. P.; Garzón, I. L.; José-Yacamán, M.; Demeler, B.; Whetten, R. L., Hidden Components in Aqueous "Gold-144" Fractionated by PAGE: High-Resolution Orbitrap ESI-MS Identifies the Gold-102 and Higher All-Aromatic Au-pMBA Cluster Compounds. *J. Phys. Chem. B* **2016**, *120* (26), 6430-6438.
36. Goswami, N.; Yao, Q.; Chen, T.; Xie, J., Mechanistic exploration and controlled synthesis of precise thiolate-gold nanoclusters. *Coord. Chem. Rev.* **2016,** *329*, 1-15.
37. Lopez, P.; Lara, H. H.; M. Mullins, S.; M. Black, D.; M. Ramsower, H.; Alvarez, M. M.; Garzón, I. L. (2018). Tetrahedral (T) Closed-Shell Cluster of 29 Silver Atoms & 12 Lipoate Ligands, $[Ag_{29}(R\text{-}\alpha\text{-}LA)_{12}]^{(3-)}$: Antibacterial and Antifungal Activity. *ACS Appl. Nano Mater.* 2018, *1* (4), 1595-1602.
38. Black, D. M.; Robles, G.; Lopez, P.; Bach, S. B. H.; Alvarez, M.; Whetten, R. L., Liquid Chromatography Separation and Mass Spectrometry Detection of Silver-Lipoate $Ag_{29}(LA)_{12}$ Nanoclusters: Evidence of Isomerism in the Solution Phase. *Anal. Chem.* **2018,** *90* (3), 2010-2017.